

## Photoabsorption of $\text{Ag}_N$ ( $N \sim 6\text{--}6000$ ) Nanoclusters Formed in Helium Droplets: Transition from Compact to Multicenter Aggregation

Evgeny Loginov,<sup>1</sup> Luis F. Gomez,<sup>1</sup> Naihao Chiang,<sup>1</sup> Avik Halder,<sup>2</sup> Nicholas Guggemos,<sup>2</sup>  
Vitaly V. Kresin,<sup>2,\*</sup> and Andrey F. Vilesov<sup>1,2,†</sup>

<sup>1</sup>*Department of Chemistry, University of Southern California, Los Angeles, California 90089, USA*

<sup>2</sup>*Department of Physics and Astronomy, University of Southern California, Los Angeles, California 90089, USA*

(Received 16 September 2010; published 10 June 2011)

$\text{Ag}_N$  clusters with up to thousands of atoms were grown in large He droplets and studied by optical spectroscopy. For  $N \leq 10^3$  the spectra are dominated by a surface plasmon resonance near 3.8 eV and a broad feature in the UV, consistent with absorption by individual metallic particles. Larger clusters reveal unexpectedly strong broad absorption at low frequencies, extending down to  $\approx 0.5$  eV. This suggests a transition from single-center to multicenter formation, in agreement with estimates of cluster growth kinetics in He droplets. Moreover, the spectra of large clusters develop a characteristic dispersion profile at 3.5–4.5 eV, indicative of the coexistence of localized and delocalized electronic excitations in composite clusters, as predicted theoretically.

DOI: 10.1103/PhysRevLett.106.233401

PACS numbers: 36.40.Mr, 36.40.Vz, 61.46.Bc, 78.67.Sc

The design and spectroscopy of noble-metal nanocluster particles and composites are active areas of basic and applied research [1]. In particular, their strong optical resonances, the possibility of localization of excitations in composite materials, and the corresponding enhancement and modification of electromagnetic resonances underpin the study of plasmonics, surface-enhanced Raman scattering, optical sensing, solar light harvesting, plasmon enhanced nanocatalysis, etc. As a consequence, there is interest in understanding and developing cluster growth and aggregation processes and in characterizing the resulting optical properties [2].

It is desirable to extend studies of composite materials to smaller, subnanometer sized grains. Granular composites of this type cannot be easily produced at the relatively high temperatures encountered in colloidal chemistry or molecular beam deposition, because of the ready coalescence of sub-nm clusters. This calls for building truly nanocomposite materials at very low temperature. Liquid He is a unique medium for aggregation as it facilitates fast thermalization of particles while allowing freedom of mobility and agglomeration [3,4].

In this Letter, we study the electronic excitation spectra of  $\text{Ag}_N$  clusters grown in superfluid He droplets, covering a wide range of droplet sizes ( $N_{\text{He}} \sim 10^4\text{--}10^7$ ), cluster sizes ( $N_{\text{Ag}} \sim 6\text{--}6000$ ), and wavelengths (IR to UV). The main finding is that, whereas the spectra of  $\text{Ag}_N$  clusters with up to hundreds of atoms are dominated by an intense resonance close to the well-known surface plasmon frequency of Ag nanoparticles, larger particles exhibit a novel feature: strong, broad absorption extending all the way into the IR region. This suggests that assembly of large nanocomposites in He droplets produces open structures, in contrast with the close-packing growth of the smaller clusters. An estimate of cluster growth kinetics supports

a transition from single-center to multicenter growth with increasing droplet size, resulting in noncompact aggregates. Moreover, the emergence of a characteristic dispersion profile in the spectra of large clusters supports the coexistence of localized and delocalized electronic excitations in composite systems, as predicted theoretically [5].

The beam apparatus is described in detail elsewhere [6]. Expansion of He gas at 20 bars through a 5  $\mu\text{m}$  diameter nozzle at  $T_0 = 10, 9.5, 9, 8,$  and  $7$  K yields droplets of initial average size of  $N_{\text{He}} \approx 2.1 \times 10^4, 2.7 \times 10^5, 2.4 \times 10^6, 1.4 \times 10^7,$  and  $4 \times 10^7$ , respectively [4]. The droplets capture Ag atoms while passing through a heated alumina oven. Further downstream, they are detected by a quadrupole mass spectrometer (QMS) hosted in a separate UHV chamber. The average number of captured Ag atoms,  $N_{\text{Ag}}$ , was estimated via attenuation of the droplet beam, as described in Ref. [6]. The flux of He atoms transported by the droplets is monitored by the partial pressure of He in the QMS chamber,  $P_{\text{He}}$ . Upon capture of Ag atoms the average droplet size decreases by an amount  $\Delta N_{\text{He}}$ , as reflected by a decrease in the partial pressure,  $\Delta P_{\text{He}}$ :  $\Delta N_{\text{He}}/N_{\text{He}} \approx \Delta P_{\text{He}}/P_{\text{He}}$ . In this work  $\Delta P_{\text{He}}/P_{\text{He}} \approx 0.7$  [6] was used in order to maximize the flux of picked-up atoms and hence the signal-to-noise ratio in the recorded spectra. Therefore  $N_{\text{Ag}}$  can be obtained as  $N_{\text{Ag}} \approx \Delta N_{\text{He}}(E_{\text{He}}/E_{\text{Ag}})$  [6], where  $E_{\text{He}} = 0.6$  meV is the binding energy of He atoms to the droplet and  $E_{\text{Ag}}$  is the energy associated with the addition of one Ag atom, i.e., the binding energy of an Ag atom to a preexisting Ag cluster. For the present accuracy, it is adequate to use  $E_{\text{Ag}} \approx 2$  eV for  $N_{\text{Ag}}$  up to several tens of atoms, which is the measured average binding energy of clusters in this size range [7], and the bulk cohesive energy  $E_{\text{Ag}} \approx 3$  eV [8] for particles with  $N_{\text{Ag}} \geq 10^2$ .

The  $\text{Ag}_N$  clusters have a broad size distribution, which is a convolution of pickup probabilities and the He droplet size distribution in the beam, the latter having a width comparable to the average size [9]. We carried out transmission electron microscope (TEM) imaging of  $\text{Ag}_N$  clusters, obtained under the same experimental conditions as in Fig. 1(e), deposited on amorphous carbon films. These measurements have shown that the clusters have an average size of  $\langle N_{\text{Ag}} \rangle = 6400$  with a mean square deviation  $\Delta N_{\text{Ag}} = 5000$  [10]. Similar agreement between the estimate and TEM measurements was also found for the clusters in Fig. 1(c). For the clusters with  $N_{\text{Ag}} \lesssim 10^2$ , the uncertainty in average size is amplified by size variations in the binding energies [7] and by the fact that TEM measurements become impractical due to low contrast.

The absorption spectra of  $\text{Ag}_N$  clusters in the range of 0.5–6 eV were obtained by beam depletion spectroscopy using a pulsed optical parametric oscillator (EKSPLA NT342/3/UV). The collimated laser beam was directed counter to the doped droplet beam, for an interaction length of about 1 m. During the 7 ns laser pulse a  $\text{Ag}_N$  cluster absorbs multiple photons. We assume that excitation of the clusters proceeds in a “multistep” manner, i.e., that the interval between successive absorption events is longer than the relaxation time of the excitation [11]. This is

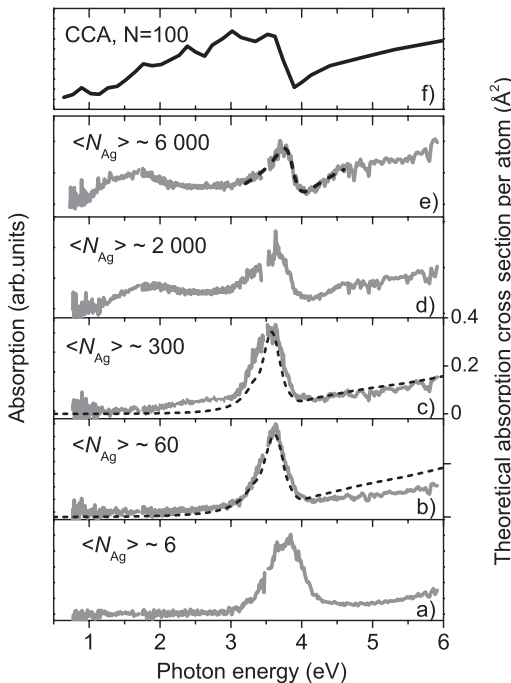


FIG. 1. Normalized photoabsorption spectra for Ag particles of different average sizes assembled by pickup in He droplets. Dashed lines in panels (b) and (c) are calculated model cross sections (right-hand scale) and in panel (e) is the fit of the dispersion profile according to the Fano formalism. The top panel (f) shows the calculated absorption spectrum of an Ag cluster-cluster aggregate from Ref. [23] (see text for details).

consistent with the  $\sim 10$  fs decay time of plasmons in Ag nanoparticles [12]. Fast relaxation of the absorbed energy results in evaporation of a sizable fraction of the host He droplet, which is monitored by the QMS as a transient fractional depletion of the  $\text{He}_2^+$  signal [3,4]. This depletion ratio is approximately proportional to the number of He atoms evaporated from the droplet and thereby to the energy released. The photoabsorption spectra discussed below have all been obtained in the linear depletion regime with an attenuated laser beam.

The measured absorption spectra are shown as solid lines in Figs. 1(a)–1(e). The spectra of the smaller clusters have a pronounced peak in the near-UV part and a prominent rise at higher energies. The peak’s maximum shifts towards lower energies with increasing cluster size: 3.8 eV, 3.7 eV, and 3.6 eV in clusters of nominal sizes  $\langle N_{\text{Ag}} \rangle \sim 6$ , 60, and 300, respectively, approaching the 3.5 eV dipolar surface plasma resonance frequency of Ag spheres [1].

Previous studies of small  $\text{Ag}_N$  clusters in He droplets reported a sharp,  $\approx 50$  meV, peak at  $\approx 4$  eV [13] in the resonant two-photon ionization spectra of  $\text{Ag}_8$ . This is distinct from the absorption spectra of size-selected  $\text{Ag}_{N=8-39}$  clusters in cryomatrices [14], which exhibit broad structures concentrated between 3 and 4.5 eV. The small  $\text{Ag}_N$  cluster data in Fig. 1 are consistent with the latter, with the spectra in Fig. 1 representing a convolution of different sizes.

Size effects in the photoabsorption of noble-metal clusters have been discussed within a model where the cluster structure is approximated by a core with a bulklike dielectric function, and a surface layer of width  $a$  in which only Drude-type  $s$ -electron screening is present [15,16]. This arises from the reduced overlap of  $s$ - and  $d$ -electron wave functions at the surface [17]. In addition, the wave functions of the outer electrons “spill out” beyond the surface by a length  $\delta$ . The dashed lines in Figs. 1(b) and 1(c) show the result of fitting the spectra with a spherical core-shell model [18,19]. The clusters with  $\langle N_{\text{Ag}} \rangle \sim 60$  and 300 are well described with the parameter choices  $a = 0.5$  Å and  $\delta = 0.2$  Å and a resonance damping factor of 20%. This is close to the parameters selected in Ref. [18] for free cluster ions [16,20]:  $a \approx 1.3$  Å, and  $\delta \approx 0$  for  $\text{Ag}_N^+$ ,  $\delta \approx 1.2$  Å for  $\text{Ag}_N^-$ . The relatively small spill-out parameter  $\delta$  for the present neutral  $\text{Ag}_N$  clusters likely derives from the exchange repulsion between the  $s$  electrons of the metal and the He matrix. The calculations also account for the broad absorption at energies  $> 5$  eV, which arises from the interaction of electron excitation modes of the core and the outer region [18,19].

The pattern changes for larger clusters, and qualitatively new features develop: (i) an intense band spanning the red and near-IR spectral ranges and (ii) a characteristic, dispersionlike profile of the excitation at 3.5–4.5 eV close to the surface plasma resonance frequency. The weakening of the UV-visible spectrum correlates with the appearance of

the IR band, as the total area under the per-atom curves in Figs. 1(a)–1(e) remains unchanged within the accuracy of the experiment.

The low-frequency band is unexpected, since extensive studies of individual Ag nanoclusters in molecular beams, on surfaces, and in colloids did not show such absorption [1]. On the other hand, certain colloidal cluster-cluster aggregates (CCAs) of nanoparticles strongly absorb in the red [1,21,22]. The changes in the spectra in Figs. 1(a)–1(e) show qualitative similarities with those obtained upon aggregation of larger Ag particles ( $R = 5\text{--}25$  nm) in colloids [21,22]. Initially, the spectrum is dominated by a plasmon peak of isolated Ag particles, which in solution has a maximum at about 3 eV. Upon extensive aggregation the intensity of the resonance decreases and the spectrum acquires a broad wing of approximately constant intensity extending down to the lowest studied excitation energy of about 1.5 eV [21,22]. The spectrum of the CCAs is determined by the strong electromagnetic interaction between the plasmon resonances of individual particles.

Model calculations show that CCAs often have a fractal structure [23], in qualitative agreement with TEM images in colloidal aggregates [22]. Figure 1(f) shows an example of the calculated absorption spectrum of a CCA consisting of 100 Ag particles, each 5 nm in diameter [23]. The spectra were calculated in the dipole approximation with renormalization of the distance between particles by a factor of about 0.8. The renormalization constant is an empirical parameter required because pure dipole-dipole theory underestimates the interaction for small interparticle distances. It is seen that the calculated spectrum extends to lower frequencies near 1 eV similarly to the experimental spectrum. Thus, the spectrum in Fig. 1(e), measured upon doping He droplets with about 6000 Ag atoms, is consistent with the CCA spectra.

To gain insight into the formation of clusters in He droplets we compare the time between two successive Ag pickup events,  $t_{n,n+1}$ , with the time required for recombination of the first two Ag atoms inside the He matrix,  $t_{\text{rec}}$ . The former can be obtained as the ratio of the time of flight of He droplets through the pickup cell (the velocity of the beam is  $\approx 200\text{--}300$  m/s [4]) to the number of captured Ag atoms. The latter time can be estimated as  $t_{\text{rec}} = V_{\text{He}}/\sigma_r \bar{v}$ , where  $V_{\text{He}}$  is the volume of the droplet,  $\sigma_r \approx 30 \text{ \AA}^2$  is the recombination cross section of Ag atoms (using the van der Waals radius of Ag), and  $\bar{v} \approx 10$  m/s is the estimated velocity of Ag atoms in the droplet assuming fast thermalization as supported by Ref. [24].

Figure 2 shows the results for  $t_{\text{rec}}$  and  $t_{n,n+1}$ , as well as the droplet parameters employed in this work. The experiment is seen to span two different modes of cluster formation. In small droplets  $t_{\text{rec}}$  is much faster than  $t_{n,n+1}$ , which results in single-center cluster growth. On the other hand, in very large droplets Ag atoms are added at a much faster rate than the time required for recombination, which

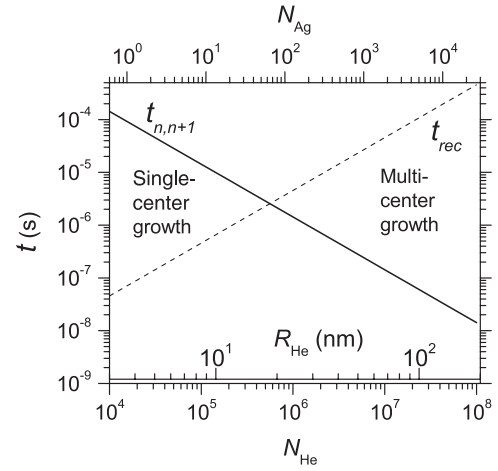


FIG. 2. Time between two successive pickup events,  $t_{n,n+1}$ , and time required for recombination of first two picked up Ag atoms,  $t_{\text{rec}}$ , versus size of He droplets,  $N_{\text{He}}$ . Corresponding droplet radius,  $R_{\text{He}}$ , and typical size of  $\text{Ag}_N$  cluster,  $N_{\text{Ag}}$ , grown within the droplet are also shown on bottom and top axes of plot, respectively.

must result in the formation of multiple smaller clusters (whose precise size is unknown at present). At longer times these coagulate into a composite. The values of  $t_{n,n+1}$  and  $t_{\text{rec}}$  are of the same order of magnitude for  $N_{\text{He}} \sim 10^6$ , corresponding to hosting  $N_{\text{Ag}} \sim 100$  atoms. Therefore this droplet size defines the lower threshold for multicenter recombination. Upon coagulation, small clusters may retain their individuality as the energy barrier associated with reconstruction into a close packed cluster is insurmountable at about 0.4 K in He droplets [4]. The appearance of the IR band for  $N_{\text{Ag}}$  greater than several hundred atoms (Fig. 1) is in good agreement with this estimated threshold for the onset of multicenter growth.

We now address feature (ii), the dispersion profile in the range of 3.5–4.5 eV, which develops in Fig. 1(d) and is fully apparent in Fig. 1(e). Its shape resembles that of a Fano resonance [25,26], which generically originates from the interaction between the narrow and broad spectra of a quantum oscillator. The dashed curve in Fig. 1(e) shows the fit of the experimental spectrum to a Fano profile,  $\sigma \propto (q\Gamma/2 + \nu - \nu_0)^2 / [(\Gamma/2)^2 + (\nu - \nu_0)^2]$ , in the vicinity of the resonance. The fit parameters are resonance energy  $\nu_0 = 3.85$  eV, width  $\Gamma = 0.30$  eV, asymmetry  $q = -1.38$ . In order to account for the changing intensity of the continuous background over the resonance we have added to the fit a linear function increasing towards higher energies. The value of  $\nu_0$  is close to the frequency of the plasmon resonance in isolated small  $\text{Ag}_N$  clusters [see Fig. 1(a)]. However, this resonance in Fig. 1(e) should not be identified with single embedded clusters, because of the formation of CCAs. The coupling strength,  $V$ , between the narrow and broad states is  $V = 0.22$  eV as obtained from the width parameter  $\Gamma = 2\pi|V|^2$  [25]. The

asymmetry parameter  $q$  reflects the transition probabilities of the resonance and the broad spectrum.

The appearance of the rather narrow resonance in CCAs is surprising in view of their expected inhomogeneity. Nevertheless, it has been predicted [5] that in disordered nanosystems, such as cluster assemblies and semicontinuous metal films, there is a coexistence of localized (due to the inhomogeneity of the clusters) and delocalized modes. Recent measurements of near-field statistics [27] and fluctuations of the local density of states [28] in percolated metal films provided support for such mode coexistence. However, there has been no direct spectroscopic confirmation. We propose that the Fano-type feature may be assigned to the interaction of the localized and delocalized modes as expected theoretically [26]. The spectrum in Fig. 1(e) also shows that both modes are luminous in a three-dimensional sample having sub-nm graininess.

Calculations indicate large differences between the spectra of fractal CCAs and compact, nonfractal aggregates [21,29]. The latter were predicted to have a similar spread of the density of states as in CCAs, but with luminous modes concentrated in a narrow spectral range close to the plasmon resonance in isolated clusters. This was rationalized in terms of certain propensity rules due to the overall spherical shape of the compact aggregates. At present the structure of the cluster aggregates formed inside the He droplets remains unknown; thus, caution should be exercised in applying theoretical spectra obtained for some distinct aggregation models. It is conceivable, for example, that the clusters obtained in He droplets may be more loosely packed (having voids) but nonfractal, thus showing a coexistence of narrow and broad modes.

In the future, detailed surface deposition experiments and x-ray scattering measurements may determine the structure of the discovered aggregates. It will be interesting to extend this work to even larger as well as to multicomponent clusters, and to investigate the application of such aggregates to surface-enhanced molecular spectroscopy at ultralow temperatures.

This work was supported by NSF Grants No. CHE-0809093 (A. V.) and No. PHY-0652534 (V. K.).

\*Corresponding author.

kresin@usc.edu

†Corresponding author.

vilesov@usc.edu

- [1] U. Kreibig and M. Vollmer, *Optical Properties of Metal Clusters* (Springer, New York, 1998).
- [2] K. D. Sattler, in *Handbook of Nanophysics*, edited by K. D. Sattler (CRC Press, Boca Raton, 2010), Vols. 2 and 6.
- [3] J. Tiggesbäumker and F. Stienkemeier, *Phys. Chem. Chem. Phys.* **9**, 4748 (2007).
- [4] J. P. Toennies and A. F. Vilesov, *Angew. Chem., Int. Ed.* **43**, 2622 (2004).
- [5] M. I. Stockman, S. V. Faleev, and D. J. Bergman, *Phys. Rev. Lett.* **87**, 167401 (2001).
- [6] V. Mozhayskiy *et al.*, *J. Chem. Phys.* **127**, 094701 (2007).
- [7] S. Krückeberg *et al.*, *J. Chem. Phys.* **110**, 7216 (1999).
- [8] B. M. Smirnov, *Reference Data on Atomic Physics and Atomic Processes* (Springer, Berlin, 2008).
- [9] U. Henne and J. P. Toennies, *J. Chem. Phys.* **108**, 9327 (1998).
- [10] E. Loginov, L. Gomez, and A. Vilesov, *J. Phys. Chem. A*, (2011).
- [11] C. Bréchnignac *et al.*, *Phys. Rev. Lett.* **68**, 3916 (1992).
- [12] J. Bosbach *et al.*, *Phys. Rev. Lett.* **89**, 257404 (2002).
- [13] T. Diederich, J. Tiggesbäumker, and K. H. Meiwes-Broer, *J. Chem. Phys.* **116**, 3263 (2002).
- [14] M. Harb *et al.*, *J. Chem. Phys.* **129**, 194108 (2008).
- [15] E. Cottancin *et al.*, *Theor. Chem. Acc.* **116**, 514 (2006).
- [16] J. Tiggesbäumker *et al.*, *Phys. Rev. A* **48**, R1749 (1993).
- [17] V. V. Kresin, *Phys. Rev. B* **51**, 1844 (1995).
- [18] V. Kasperovich and V. V. Kresin, *Philos. Mag. B* **78**, 385 (1998). (In Fig. 2  $\epsilon_1$  and  $\epsilon_2$  were accidentally interchanged.)
- [19] J. Lermé, *Eur. Phys. J. D* **10**, 265 (2000).
- [20] J. Tiggesbäumker, L. Köller, and K. H. Meiwes-Broer, *Chem. Phys. Lett.* **260**, 428 (1996).
- [21] V. A. Markel *et al.*, *Phys. Rev. B* **53**, 2425 (1996).
- [22] S. V. Karpov *et al.*, *J. Chem. Phys.* **125**, 111101 (2006).
- [23] V. A. Markel *et al.*, *Phys. Rev. B* **70**, 054202 (2004).
- [24] A. Braun and M. Drabbels, *J. Chem. Phys.* **127**, 114303 (2007).
- [25] U. Fano, *Phys. Rev.* **124**, 1866 (1961).
- [26] B. Luk'yanchuk *et al.*, *Nature Mater.* **9**, 707 (2010).
- [27] K. Seal *et al.*, *Phys. Rev. Lett.* **97**, 206103 (2006).
- [28] V. Krachmalnicoff *et al.*, *Phys. Rev. Lett.* **105**, 183901 (2010).
- [29] Z. Naeimi and M. F. Miri, *Phys. Rev. B* **80**, 224202 (2009).